SPECIAL TOPIC — Smart design of materials and design of smart materials

Impeded thermal transport in aperiodic BN/C nanotube superlattices due to phonon Anderson localization

Luyi Sun(孙路易), Fangyuan Zhai(翟方园), Zengqiang Cao(曹增强), Xiaoyu Huang(黄晓宇), Chunsheng Guo(郭春生), Hongyan Wang(王红艳), and Yuxiang Ni(倪宇翔)†

School of Physical Science and Technology, Southwest Jiaotong University, Chengdu 610031, *China*

(Received 31 December 2022; revised manuscript received 5 February 2023; accepted manuscript online 8 February 2023)

Anderson localization of phonons is a kind of phonon wave effect, which has been proved to occur in many structures with disorders. In this work, we introduced aperiodicity to boron nitride/carbon nanotube superlattices (BN/C NT SLs), and used molecular dynamics to calculate the thermal conductivity and the phonon transmission spectrum of the models. The existence of phonon Anderson localization was proved in this quasi one-dimensional structure by analyzing the phonon transmission spectra. Moreover, we introduced interfacial mixing to the aperiodic BN/C NT SLs and found that the coexistence of the two disorder entities (aperiodicity and interfacial mixing) can further decrease the thermal conductivity. In addition, we also showed that anharmonicity can destroy phonon localization at high temperatures. This work provides a reference for designing thermoelectric materials with low thermal conductivity by taking advantage of phonon localization.

Keywords: Anderson localization, phonons, nanotube superlattices, thermal conductivity

PACS: 63.20.Pw, 63.20.–e, 63.22.Gh, 44.10.+i **DOI:** 10.1088/1674-1056/acb9e7

1. Introduction

Thermoelectric (TE) material is a kind of functional materials which takes advantage of the Seebeck effect to realize the direct conversion between thermal energy and electrical energy.[1] The advent of thermoelectric materials brings hope for the sustainable development of energy in the future.[2] However, the application of thermoelectric materials is limited by their low efficiency. To achieve high TE energy conversion efficiency, low thermal conductivity (κ) is desired since the energy conversion efficiency (characterized by the figure of merit, ZT) is inversely proportional to thermal transport. It has been reported that reducing the lattice thermal conductivity is the primary approach for promoting the thermoelectric properties of materials.[3–7] Actually, the thermal property is of great significance to various materials, including TE material, thermal interface materials, energetic materials, plasma facing materials, *et al.*[8–10]

Fortunately, the physical properties can be tuned by the structural change of materials.[11–13] With the development of nanotechnology, low thermal conductivity can be achieved by the nanostructural design of materials, taking advantages of the quantum effects, classical size effects and interface effects.[14–18] Phonons are a kind of boson with wave–particle duality. Utilizing the phonon particle nature (incoherence), the propagation of phonons can be impeded through phonon scattering. Previous studies show that structures such as zero-dimensional point defects,[19,20] one-dimensional dislocations[21,22] and two-dimensional interfaces[23] can lead to phonon scattering thus decreasing the thermal conductivity.

On the other hand, the lattice thermal conductivity can be manipulated by using the phonon wave effects (coherence) such as the phonon resonance[24–26] and phonon interference.[27,28] The latter can be derived from the disturbance of the coherent phonons by structural disorders, causing backscattering of coherent phonons,[29] a phenomenon known as phonon Anderson localization.[30] Phonon Anderson localization has been observed in a series of systems, including GaAs/AlAs superlattices with ErAs nanodots,[31] silicon nanowires,[18,32] nanoscale 3D Si phononic crystal with spherical pores,[33] graphene/h-BN superlattices,[34] and Si/Ge superlattices.[35,36] Taking graphene/h-BN superlattices (Gr/h-BN SLs) as examples, it was reported that the thermal transport can be largely impeded by disorder entities including randomized layer thicknesses (aperiodicity, ap)[37] and interfacial mixing.[34,38]

In spite of the aforementioned studies, phonon Anderson localization has rarely been reported for the quasi one-dimensional nanotube systems, which represents an important type of nanostructure as well as a potential TE material.[39] It raises a question whether the disorder entities such as aperiodicity and interfacial mixing can still induce phonon Anderson localization in nanotubes. The answer to this question is obscure because for systems with the same length, the hollow nature of nanotubes leads to much fewer atoms compared with nanowires and two-dimensional materials, providing limited spaces for disorders such as random alloys.

In this study, by using molecular dynamics simulations, we investigate the thermal transport in boron nitride/carbon

†Corresponding author. E-mail: yuxiang.ni@swjtu.edu.cn

© 2023 Chinese Physical Society and IOP Publishing Ltd

nanotube superlattices (BN/C NT SLs). By setting randomized layer thicknesses and interfacial mixing, different disorder entities were introduced to BN/C NT SLs. The exponential decay of phonon transmission spectra with the length of disordered medium corroborates the existence of phonon Anderson localization, which is the cause of the reduced thermal conductivity in the relevant structures. Meanwhile, the coexistence of the two disorder entities (aperiodicity and interfacial intermixing) can further decrease the thermal conductivity of BN/C NT SLs.

The structure of this paper is as follows. In Section 2, we introduce the atomistic models of BN/C NT SLs used in the simulations, and the methods for the thermal conductivity and phonon transmission spectra calculations. In Section 3, we show the thermal conductivity and phonon transmission spectra results, and the Anderson localization is analyzed. Finally, the main findings of this work are summarized in Section 4.

2. Methods

2.1. Atomistic models

First, we constructed a periodic BN/C NT SL of 10 periods with a length of 29.76 nm (Fig. 1(a)). The chirality index of the periodic BN/C NT SL is (10,10) and the C–C, C–B, and B–N bond lengthes were all set as 1.43 Å. The perimeter (C) of the BN/C NT SLs is[40]

$$C = d_t\pi = \sqrt{3}a\sqrt{m^2+n^2+mn}, \tag{1}$$

where d_t is the diameter of the BN/C NT SLs, a is the bond length (1.43 Å) and (m, n) is the chirality index (10,10). So, we can define the volume (V) of the BN/C NT SLs as[41]

$$\begin{aligned} V &= LC\bar{\delta} \\ &= LC(50\%\delta_C + 25\%\delta_B + 25\%\delta_N), \end{aligned} \tag{2}$$

where L is the length of the BN/C NT SLs and δ_C, δ_B, δ_N are the van der Waals diameters of carbon atoms (3.40 Å), nitrogen atoms (3.10 Å), boron atoms (3.84 Å), respectively.

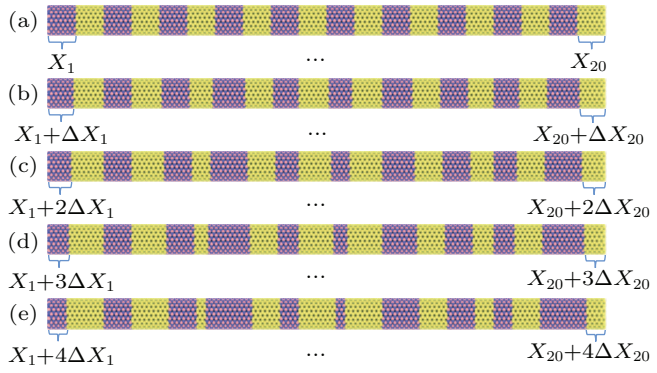


Fig. 1. Atomistic models of BN/C NT SLs: (a) periodic, (b)–(e) aperiodic.

We mark the length of each CNT (BN) section as X_1, X_2, ..., X_{20}. For periodic NT SL, $X_1 = X_2 = \cdots = X_{20} = 14.88$ Å. Then, we randomly changed the length of each section to construct aperiodic BN/C NT SLs, while keeping the total length unchanged. The ratio of the atomic species also remained unaltered. For example, as shown in Fig. 1(b), the changed length of each section is ΔX_1, ΔX_2, ..., ΔX_{20}, respectively (ΔX_n was randomly chosen from 0 Å, ±1.24 Å, ±2.48 Å; $n = 1, 2, 3, \ldots, 20$). Based on the model shown in Fig. 1(b), we continued to construct three more aperiodic BN/C NT SLs (Figs. 1(c), 1(d), 1(e)) with increasing section length variations of $2\Delta X_n$, $3\Delta X_n$, and $4\Delta X_n$, respectively. Thus, larger section length variation indicates more severe disorder in the system.

Then we constructed two structures based on the aperiodic BN/C NT SL shown in Fig. 2(a). One is a system with serrated interfaces (Fig. 2(b)), and the other one has rough interfaces (Fig. 2(c)). The "serrated interfaces" exhibit regular notched shape, while the "rough interfaces" bear random exchange of the atomic species, which were realized by randomly replacing the C (BN) atoms by BN (C) atoms, while the ratio of the atomic species was kept constant. The motivation for studying those two structures was to compare the impact of the regular interface shape and the random disordered interface shape on the thermal transport, as the interfacial structure is crucial to the interfacial thermal resistance.[42] The length of the serrated interfaces and that of the rough interfaces were both set to 4.96 Å, as indicated in Figs. 2(b) and 2(c).

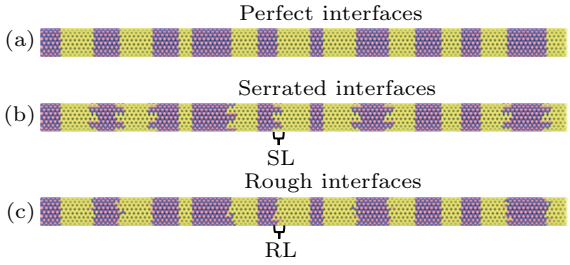


Fig. 2. Atomistic models of aperiodic BN/C NT SLs with different interfaces: (a) perfect interfaces, (b) serrated interfaces, and (c) rough interfaces.

Models with different central lengths were built for the phonon transmission calculations from non-equilibrium molecular dynamics (NEMD) simulations. Sections with 2 nm in length at the two ends of the tubes were fixed, while the adjacent sections of 13 nm were set as hot and cold reservoirs, respectively.

2.2. Thermal conductivity calculation

The thermal conductivities of the models shown in Figs. 1 and 2 were calculated from equilibrium molecular dynamics (EMD) simulations by using the LAMMPS software package.[43] The thermal conductivity κ_z along the direction perpendicular to the interface (z-direction) was calculated

from the Green–Kubo formula[44]

$$\kappa_z = \frac{V}{k_B T^2}\int_0^{+\infty}\langle j_z(t) j_z(t)\rangle \mathrm{d}t, \tag{3}$$

where T, V, and k_B are the temperature, volume, and Boltzmann constant, respectively. The $j_z(t)$ is heat flux along the z-direction and the angular brackets denote the ensemble average.

In the software, we set the MD time step to 0.5 fs, and periodic boundary conditions were applied in the axial direction. The Tersoff potential was adopted to describe the atomic interactions.[45] First, we relaxed the initial structures by using the conjugate gradient energy minimization algorithm. Then, the structures were evolved in the canonical ensemble (NVT) for 200 ps in order to impose a temperature of 300 K. After that, MD runs with lengths equal to 160 ps in the microcanonical ensemble (NVE) were performed to calculate the heat flow along the z-direction. We carried out 10 independent MD simulations to get the ensemble average in the angular brackets, based on which κ_z was calculated.

2.3. Phonon transmission spectra calculation

The method proposed by Saaskilahti *et al.*[46,47] was used to calculate the phonon transmission spectra of BN/C NT SLs from non-equilibrium molecular dynamics. The frequency-decomposed heat flow between any two atoms i and j can be expressed as

$$q_{i\to j}(\omega) \approx -\frac{2}{t_{\mathrm{simu}}\omega}\sum_{\alpha,\beta\in\{x,y,z\}}\mathrm{Im}\langle \hat{v}^P \alpha_i(\omega) K_{ij}^{\alpha\beta}\hat{v}_j^{\beta}(\omega)\rangle, \tag{4}$$

where ω denotes the frequency and t_{simu} is the simulation time. $\hat{v}_i^{\alpha}(\omega)$ and $\hat{v}_j^{\beta}(\omega)$ are the velocities of atoms i and j in the α and β directions after Fourier transforms, respectively. $K_{ij}^{\alpha\beta}$ is the force constant matrix which denotes the force constant between atom i and atom j. Assuming a virtual interface where the atoms on the left and right sides of the interface belong to the atomic groups L and R, respectively. Then the heat current across the interface can be obtained by summing over atoms in each group:

$$q(\omega) = \sum_{i\in\mathrm{L}}\sum_{j\in\mathrm{R}} q_{i\to j}(\omega). \tag{5}$$

With the heat current, the phonon transmission function can be defined as

$$T(\omega) = \frac{q(\omega)}{k_B \Delta T}, \tag{6}$$

where ΔT is the temperature difference of the two thermal baths in NEMD simulations. To calculate $\hat{v}_i^{\alpha}(\omega)$ and $\hat{v}_j^{\beta}(\omega)$, the Langevin heat baths at $T+\Delta T/2$ and $T-\Delta T/2$ were imposed, as shown in Fig. 3(a). The MD time step was set to 1 ps. The average heat bath temperature was fixed at $T = 300$ K (500 K, 800 K) and ΔT was set to 60 K. Temperatures were imposed by the Langevin thermostat, which outperforms the Nosé–Hoover (chain) thermostat in NEMD simulations because of its stochastic and local nature.[48] We calculated $K_{ij}^{\alpha\beta}$ by LAMMPS using the finite difference method: fix atom j, move atom i along $\pm x$, $\pm y$, $\pm z$ directions, respectively by a small distance ($\Delta = 0.01$ Å). After each displacement, we can calculate the force on atom j in atomic groups L and R. As a result, the force constant matrix can be expressed as

$$K_{ij}^{\alpha\beta} = \frac{F_j^{\beta-} - F_j^{\beta+}}{2\Delta}, \tag{7}$$

where $F_j^{\beta-}$ and $F_j^{\beta+}$ are the forces on atom j in the β direction when atom i moves to the $-\alpha$ and $+\alpha$ directions. With $\hat{v}_i^{\alpha}(\omega)$, $\hat{v}_j^{\beta}(\omega)$ and $K_{ij}^{\alpha\beta}$, $T(\omega)$ can be obtained.

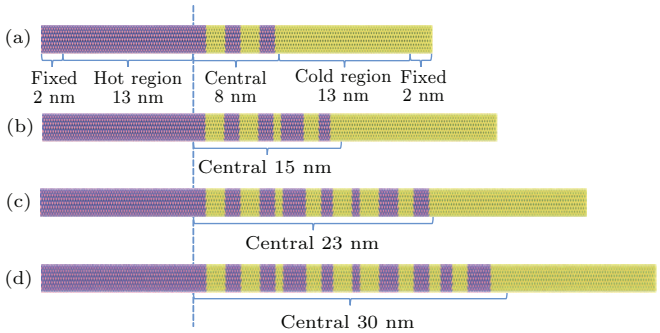


Fig. 3. Atomistic models used in the phonon transmission calculations from NEMD.

3. Results and discussion

3.1. Thermal conductivity of BN/C NT SLs

Figure 4 shows the calculated thermal conductivities of the BN/C NT SLs of different section length variations at 300 K. Also shown in the figure are the thermal conductivities of the aperiodic BN/C NT SLs with serrated interface and rough interface (red circle and blue triangle).

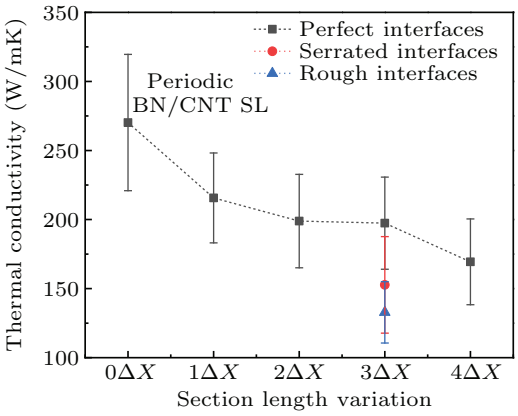


Fig. 4. Thermal conductivity of different BN/C NT SLs at 300 K.

As shown in Fig. 4, the κ_z of the periodic BN/C NT SL is around 270 W/mK. When disorder is introduced to the system, a sizable reduction in κ_z is observed, and it continues to decrease as the section length variation increases. This phenomenon indicates that the phonon propagation is more significantly suppressed as the disorder degree increases. For example, when the section length variation reaches $4\Delta X$, a 37.4% reduction in κ_z is realized compared with the system without disorder. Except for the section length variation, the interface structure also has obvious impact on κ_z. As shown in Fig. 4, the serrated interfaces and the rough interfaces further reduce the thermal conductivity.

3.2. Phonon analyses of aperiodic BN/C NT SLs at different temperatures

To elucidate the physical mechanism underling the impeded thermal transport in BN/C NT SLs, the corresponding phonon transmission spectra were calculated. Figure 5 shows the phonon transmission spectra of the aperiodic BN/CNT SL with different system lengths at different temperatures. From Fig. 5(a), the ballistic phonon transport can be observed below ~ 1 THz. The transmission of the low-frequency phonons (below 1 THz) does not change obviously as the length of the aperiodic BN/C NT SL increases. This is because these phonons bear long-wavelength, and cannot be scattered effectively while propagating through even the entire length of a superlattice.[31] In general, the phonon transmission spectrum decreases with the increase of the length of the superlattice, except for the frequencies below 1 THz and around 35 THz.

Because of the interference of the phonon waves reflected due to the back scatterings at the random interfaces, phonon localization may occur in this structure. Therefore, the localization regime can be established, featured by the exponential decay of phonon transmission[36]

$$T(\omega) = T_0(\omega) \cdot \mathrm{e}^{-L/\xi}, \tag{8}$$

where $T(\omega)$ is the phonon transmission coefficient of the structure, L is the system length, and ξ is the localization length. By fitting $T(\omega)$ of Figs. 5(a)–5(c) with Eq. (8), the frequency-resolved phonon localization length at different temperatures can be obtained. We use the coefficient of determination R^2 to evaluate the degree of fitting. The coefficient of determination R^2 equal to 1 means that the model perfectly fits the data.[49] For systems at 300 K, we find that most of the fittings can achieve very high values of R^2 (> 0.95), which corroborates the existence of phonon Anderson localization in the aperiodic BN/C NT SL at 300 K. In Fig. 5(d), we summarize the localization length corresponding to the frequency with R^2 greater than 0.99 for the systems at different temperatures. It can be seen that the population of localized modes decreases with temperature, as the anharmonicity will destroy phonon localization at high temperatures.[50,51] It would be interesting to note that some random multilayer structures were reported to exhibit enhanced thermal transport than the SL counterpart even in the presence of phonon localization.[52]

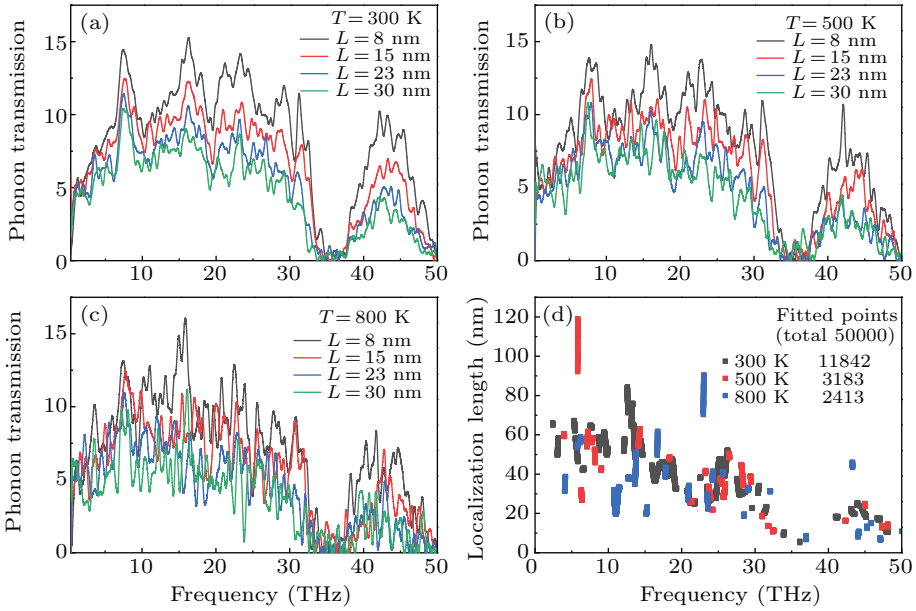


Fig. 5. Phonon transmission spectra and phonon localization length of the aperiodic BN/C NT SL at different temperatures.

3.3. Phonon analyses of aperiodic BN/C NT SLs with different interfaces

The phonon transmission spectra of the aperiodic BN/C NT SL with serrated interfaces and rough interfaces were evaluated at 300K. According to Fig. 6(a), it can be obviously seen that the phonon transmission spectra of the serrated and rough interfaces are lower than that of the perfect interfaces at 300 K. This means both serrated interfaces and rough interfaces ob-

struct heat transfer. We also fitted the phonon transmission spectrum with the exponential decay model and plotted the localization length in Fig. 6(d). It can be inferred that fewer frequencies meet the fitting conditions ($R^2 > 0.99$) in aperiodic BN/C NT SL with serrated interfaces than that in aperiodic BN/C NT SL with perfect interfaces. That is to say, the serrated interfaces weaken the phonon localization. Therefore, the reduction of thermal conductivity for serrated interfaces is due to the enhanced phonon scattering rather than phonon localization.[53] Unlike serrated interfaces, the rough interfaces somewhat increase the disorder of the system, and the phonon localization is enhanced.[34] This means that the superposition of the two types of disorders (aperiodic and rough interface) can work together to decrease the thermal conductivity even further.

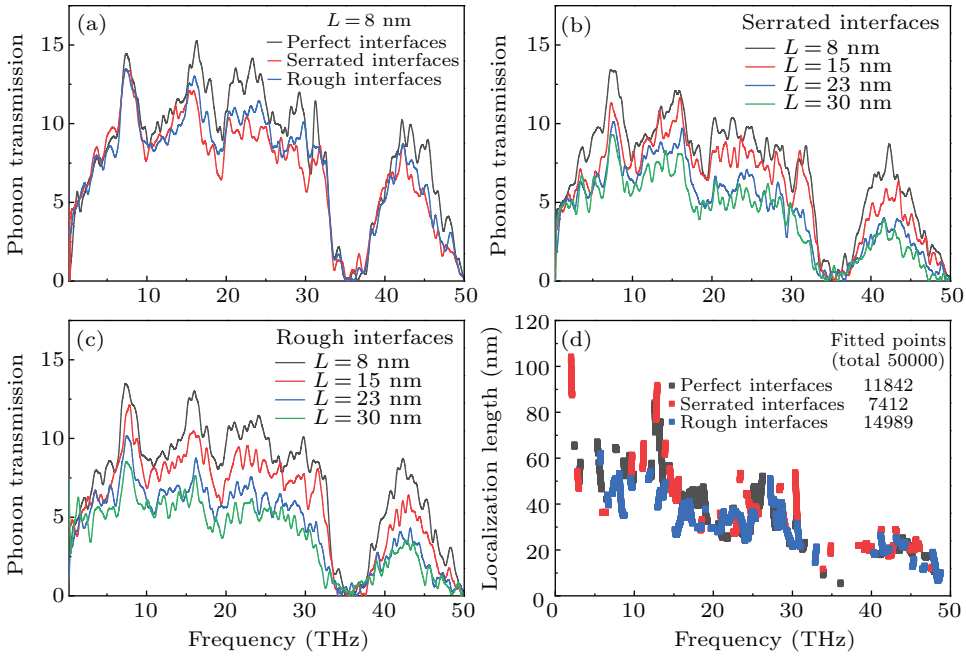


Fig. 6. Phonon transmission spectra and phonon localization length of the aperiodic BN/C NT SL with different interfaces at 300 K.

4. Conclusion

To sum up, by performing molecular dynamics simulations, we calculated and compared the thermal conductivity of different aperiodic BN/C NT SLs with different interfaces. Then we demonstrated the existence of phonon localization in aperiodic BN/C NT SLs by analyzing the phonon transmission spectra. We also found that the anharmonicity will destroy phonon localization at high temperatures. The coexistence of the two distinct disorder entities (aperiodicity and interfacial intermixing) can further enhance the phonon localization and decrease thermal conductivity. This work provides a new idea for the design of thermoelectric materials with low thermal conductivity by using disordered structures.

References

[1] Tritt T M, Böttner H and Chen L D 2008 *MRS Bull.* **33** 366

[2] Chu S and Majumdar A 2012 *Nature* **488** 294

[3] Kim S I, Lee K H, Mun H A, Kim H S, Hwang S W, Roh J W, Yang D J, Shin W H, Li X S, Lee Y H, Snyder G J and Kim S W 2015 *Science* **348** 109

[4] Biswas K, He J, Blum I D, Wu C I, Hogan T P, Seidman D N, Dravid V P and Kanatzidis M G 2012 *Nature* **489** 414

[5] Li J, Chen Z W, Zhang X Y, Yu H L, Wu Z H, Xie H Q, Chen Y and Pei Y Z 2017 *Adv. Sci.* **4** 1700341

[6] Li W, Zheng L, Ge B, Lin S, Zhang X, Chen Z, Chang Y and Pei Y 2017 *Adv. Mater.* **29** 1605887

[7] Zhao L D, Lo S H, Zhang Y, Sun H, Tan G, Uher C, Wolverton C, Dravid V P and Kanatzidis M G 2014 *Nature* **508** 373

[8] Due J and Robinson A J 2013 *Appl. Therm. Eng.* **50** 455

[9] Liu W H, Liu Q J, Zhong M, Gan Y D, Liu F S, Li X H and Tang B 2022 *Acta Mater.* **236** 118137

[10] Huang X Y, Huang J, Cao Z Q, Wang H Y, Zhang X, Xu Y H and Ni Y X 2022 *J. Nucl. Mater.* **570** 153981

[11] Zhang D B, Wang K, Chen S, Zhang L F, Ni Y X and Zhang G 2023 *Nanoscale* **15** 1180

[12] Zhou Y G, Xiong S Y, Zhang X L, Volz S and Hu M 2018 *Nat. Commun.* **9** 4712

[13] Wang H Y, Cheng Y J, Nomura M, Volz S, Donadio D, Zhang X H and Xiong S Y 2021 *Phys. Rev. B* **103** 085414

[14] Hicks L D and Dresselhaus M S 1993 *Phys. Rev. B* **47** 16631

[15] Dresselhaus M S, Chen G, Tang M Y, Yang R G, Lee H, Wang D Z, Ren Z F, Fleurial J P and Gogna P 2007 *Adv. Mater.* **19** 1043

[16] Venkatasubramanian R, Siivola E, Colpitts T and O'Quinn B 2001 *Nature* **413** 597

[17] Chen Z, Zhang X and Pei Y 2018 *Adv. Mater.* **30** 1705617

[18] Ma D, Arora A, Deng S, Xie G, Shiomi J and Yang N 2019 *Mater. Today Phys.* **8** 56

[19] Li W, Lindsay L, Broido D A, Stewart D A and Mingo N 2012 *Phys. Rev. B* **86** 174307

[20] Pei Y Z, Shi X Y, LaLonde A, Wang H, Chen L D and Snyder G J 2011 *Nature* **473** 66

[21] Ni Y X, Xiong S Y, Volz S and Dumitric T 2014 *Phys. Rev. Lett.* **113** 124301

[22] Xiong S Y, Ma J, Volz S and Dumitricš T 2014 *Small* **10** 1756

[23] Joshi G, Lee H, Lan Y, Wang X, Zhu G, Wang D, Gould R W, Cuff D C, Tang M Y, Dresselhaus M S, Chen G and Ren Z 2008 *Nano Lett.* **8** 4670

[24] Honarvar H and Hussein M I 2016 *Phys. Rev. B* **93** 081412

[25] Xiong S Y, Sääskilahti K, Kosevich Y A, Han H X, Donadio D and Volz S 2016 *Phys. Rev. Lett.* **117** 025503

[26] Li K Q, Cheng Y J, Wang H Y, Guo Y Y, Zhang Z W, Bescond M, Nomura M, Volz S, Zhang X H and Xiong S Y 2022 *Int. J. Heat Mass Transf.* **183** 122144

[27] Liao B L and Chen G 2015 *MRS Bull.* **40** 746

[28] Jiang P F, Ouyang Y L, Ren W J, Yu C Q, He J and Chen J 2021 *APL Mater.* **9** 040703

[29] Ni Y X and Volz S 2021 *J. Appl. Phys.* **130** 190901

[30] Anderson P W 1958 *Phys. Rev.* **109** 1492

[31] Luckyanova M N, Mendoza J, Lu H, Song B, Huang S, Zhou J, Li M, Dong Y, Zhou H, Garlow J, Wu L, Kirby B J, Grutter A J, Puretzky A A, Zhu Y, Dresselhaus M S, Gossard A and Chen G 2018 *Sci. Adv.* **4** eaat9460

[32] Ma D K, Ding H R, Meng H, Feng L, Wu Y, Shiomi J and Yang N 2016 *Phys. Rev. B* **94** 165434

[33] Yang L, Yang N and Li B 2014 *Nano Lett.* **14** 1734

[34] Ni Y X, Zhang H G, Hu S, Wang H Y, Volz S and Xiong S Y 2019 *Int. J. Heat Mass Transf.* **144** 118608

[35] Hu R J and Tian Z T 2021 *Phys. Rev. B* **103** 045304

[36] Guo Y Y, Bescond M, Zhang Z W, Xiong S Y, Hirakawa K, Nomura M and Volz S 2021 *APL Mater.* **9** 091104

[37] Ma T F, Lin C T and Wang Y 2020 *2D Mater.* **7** 035029

[38] Zhang H G, Xiong S Y, Wang H Y, Volz S and Ni Y X 2019 *Europhys. Lett.* **125** 46001

[39] Lee H R, Furukawa N, Ricco A J, Pop E, Cui Y and Nishi Y 2021 *Appl. Phys. Lett.* **118** 173901

[40] Dresselhaus M S and Eklund P C 2000 *Adv. Phys.* **49** 705

[41] Bai D 2011 *Fuller. Nanotub. Carbon Nanostructures* **19** 271

[42] Chen J, Xu X F, Zhou J and Li B W 2022 *Rev. Mod. Phys.* **94** 025002

[43] Plimpton S 1995 *J. Comput. Phys.* **117** 1

[44] Kubo R, Toda M and Hashitsume N 1985 *Statistical Physics II* (Heidelberg: Springer Berlin) pp. 203–263

[45] Tersoff J 1989 *Phys. Rev. B* **39** 5566

[46] Sääskilahti K, Oksanen J, Tulkki J and Volz S 2014 *Phys. Rev. B* **90** 134312

[47] Sääskilahti K, Oksanen J, Volz S and Tulkki J 2015 *Phys. Rev. B* **91** 115426

[48] Li Z, Xiong S Y, Sievers C, Hu Y, Fan Z Y, Wei N, Bao H, Chen S D, Donadio D and Ala-Nissila T 2019 *J. Chem. Phys.* **151** 234105

[49] Nagelkerke N J D 1991 *Biometrika* **78** 691

[50] Liu Y and He D H 2017 *Phys. Rev. E* **96** 062119

[51] Wang Y, Huang H X and Ruan X L 2014 *Phys. Rev. B* **90** 165406

[52] Yu C Q, Ouyang Y L and Chen J 2022 *Front. Phys.* **17** 53507

[53] Mao J, Wang Y M, Liu Z H, Ge B H and Ren Z F 2017 *Nano Energy* **32** 174